

<https://doi.org/10.15407/ujpe67.7.536>

R.S. BREZVIN,<sup>1</sup> O.YA. KOSTETSKYI,<sup>1</sup> V.YO. STADNYK,<sup>1</sup> P.A. SHCHEPANSKYI,<sup>1,2</sup>  
O.M. HORINA,<sup>2,3</sup> M.YA. RUDYSH,<sup>1,2,4,5</sup> A.O. SHAPRAVSKYI<sup>1</sup>

<sup>1</sup> Ivan Franko National University of Lviv

(19, Drahomanova Str., Lviv 79023, Ukraine; e-mail: vasylstadnyk@ukr.net)

<sup>2</sup> Lviv Polytechnic National University

(12, Bandery Str., Lviv 79013, Ukraine)

<sup>3</sup> Lviv State University of Life Safety

(35, Kleparivska Str., Lviv 79007, Ukraine)

<sup>4</sup> Jan Długosz University in Częstochowa

(13/15, Al. Armii Krajowej, Częstochowa 42-201, Poland)

<sup>5</sup> Lesya Ukrainka Volyn National University

(9, Potapova Str., Lutsk 43025, Ukraine)

## DILATOMETRIC STUDY OF $\text{LiNH}_4\text{SO}_4$ CRYSTALS WITH MANGANESE IMPURITY

---

*A crystal of lithium-ammonium sulfate with a manganese impurity of 5% has been synthesized and its structural parameters (the atomic coordinates and the unit cell parameters) have been specified. The introduction of the impurity was found to change the absolute values of the thermal expansion coefficient  $\Delta l/l_0$ , but not its behavior. Furthermore, a negative thermal expansion along the specimen Z direction is revealed near the phase transition point. It is shown that the introduction of the impurity shifts the phase transition point toward lower temperatures from 461 K (for the pure crystal) to 455.7 K (for the impurity-doped crystal), reduces the linear expansion coefficient  $\alpha_i$  in the interval of positive thermal expansion, increases it in the interval of negative thermal expansion, and extends the temperature interval, where the thermal expansion coefficient is negative. Indicative surfaces of the thermal expansion coefficient in the ferroelectric and paraelectric phases have been plotted. The independent study and the verification of the phase transition have been performed with the use of the method of differential thermal analysis.*

*Keywords:* crystal, impurity, thermal expansion, phase transition, differential thermal analysis.

### 1. Introduction

Recently, the considerable attention has been paid to the study of the physical properties of crystals belonging to the family of sulfates  $\text{ABSO}_4$  ( $A, B = \text{Li}, \text{Na}, \text{K}, \text{Rb}, \text{Cs}, \text{or } \text{NH}_4$ ) and possessing a number of interesting physical properties (ferroelectricity and

ferroelasticity, second-harmonic generation, fast ionic conductivity at high temperatures, and others). It is worth noting that the cation substitution in the crystal gives rise to substantial changes in the sequence of phase transitions (PTs). For the examined crystals, the PT is of the order-disorder type, being mainly associated with the dynamics and orientation of the  $\text{SO}_4$  tetrahedra, whereas the cations  $A$  and  $B$  are responsible for the PT character.

Typical representatives of this class are lithium-ammonium sulfate (LAS) crystals  $\text{LiNH}_4\text{SO}_4$ . Depen-

---

© R.S. BREZVIN, O.YA. KOSTETSKYI,  
V.YO. STADNYK, P.A. SHCHEPANSKYI,  
O.M. HORINA, M.YA. RUDYSH,  
A.O. SHAPRAVSKYI, 2022

ding on their growth conditions, they can exist in two modifications:  $\alpha$  and  $\beta$ . For pure  $\text{LiNH}_4\text{SO}_4$  crystals of  $\beta$ -modification ( $\beta$ -LAS), their optical, dielectric, elastomechanical, and thermal properties together with the influence on them of hydrostatic or uniaxial pressure, as well as such phenomena as nuclear magnetic resonance (NMR), Brillouin scattering, and so forth, have been studied [1–12]. In particular, those crystals demonstrate a number of interesting PTs. At atmospheric pressure and the temperature  $T_1 = 461$  K, the  $\beta$ -LAS crystal undergoes a PT from the paraelectric  $Pm\bar{c}n$  phase to the ferroelectric  $Pc2_1n$  one. In the high-temperature phase, the  $\text{SO}_4$  and  $\text{LiO}_4$  tetrahedra have common angles and form pseudo-hexagonal six-link rings oriented perpendicularly to the  $c$ -axis. The  $\text{NH}_4$  groups are located at the centers of large interlayer cavities created by those rings. After the transition from the paraelectric phase to the ferroelectric one, the  $\text{SO}_4$  tetrahedra, which were in two configurations, become ordered in either of them with a probability of 0.9. A characteristic feature of the ferroelectric phase is the existence of a domain structure along the orthorhombic axis  $b$  [13–21].

In the course of dilatometric studies of the pure  $\beta$ -LAS crystal, regions with zero and negative thermal expansions (NTEs) were revealed [23]. NTE can be found in functional materials of various types. It is important, first of all, for their practical application, since most of the available industrial-grade materials have positive thermal expansion coefficients, which negatively affects their performance at temperatures higher than the “extreme” ones. The application of materials with zero and negative thermal expansions can be useful to prevent the damage to composite materials, for example, computer chip components subjected to sudden temperature changes [23, 24].

The introduction of impurities is an effective tool for varying the physical parameters of crystals: the shift of PT points, the extension (narrowing) of the temperature interval of phase existence, and the changes of the temperature intervals with zero and negative thermal expansions of the crystals.

Previous studies of the absorption spectra of LAS crystals with impurities of copper ions in an interval of 600–1350 nm revealed the appearance of three new peaks at about 7500, 10000, and 12500  $\text{cm}^{-1}$ , whereas the band at 12070  $\text{cm}^{-1}$  was found shifted toward short waves by 66  $\text{cm}^{-1}$  in comparison with the pure crystal [25].

By analyzing the temperature,  $T$ , dependence of the specific heat capacity  $C_p$ , the influence of a doping of LAS crystals with metal  $\text{Cs}^+$  ions on the position of PT points was studied [3, 22, 25, 32] and substantial changes of this parameter were revealed. In particular, the  $C_p(T)$  peak associated with the PT becomes sharper and shifts toward lower temperatures as the impurity concentration increases. The cited authors assumed that the introduction of the Cs impurity induces the expansion of the critical temperature interval, changes the thermodynamic parameters, and decreases the excitation energy of dipoles.

Doping was found to bring about two opposite effects [26–29]. If the impurity concentration is low, an insignificant misorientation of domain walls may take place near a defect depending on its polarity, which changes the domain wall energy and, accordingly, the energy of dipoles. In the case of high concentrations, the domain structure can become squeezed, which reduces the domain wall energy and, accordingly, the energy of dipoles.

Earlier, the influence of the impurity of the transition metal copper (Cu) on the optical-electronic parameters of isomorphous  $\text{K}_2\text{SO}_4$  crystals was studied [30–32]. It was found that the introduction of the impurity decreases the magnitudes of the refractive indices  $n_i$ , changes the magnitudes of birefringence, enhances the temperature dependence  $\Delta n_i(T)$ , slightly decreases the thermal expansion  $\Delta l/l_i$ , substantially changes the magnitude of a jump in the course of PT, and shifts the PT point toward lower temperatures.

No corresponding works for LAS crystals have been carried out so far. Therefore, there arose a necessity to determine the impurity influence on the dilatometric parameters of those crystals. In this work, the effect of the manganese (Mn) impurity on the thermal expansion and the position of the PT point of LAS crystals is studied in order to elucidate the possibility of controlling the physical properties of those crystals.

## 2. Experimental Technique

The studied  $\text{LiNH}_4\text{SO}_4:\text{Mn}$  crystals of  $\beta$ -modification were grown from an aqueous solution by slowly evaporating the solvent [33]. The growth took place at a constant temperature of 318 K, which was maintained by a thermostat with an accuracy of 0.1 K. The initial compounds were chemically

pure salts of lithium sulfate  $\text{Li}_2\text{SO}_4$  and ammonium sulfate  $(\text{NH}_4)_2\text{SO}_4$  in the equimolar ratio,



and manganese sulfate crystal hydrate  $\text{MnSO}_4 \cdot 5\text{H}_2\text{O}$ . To ensure the highest quality of the obtained crystals, the compounds were recrystallized several times. Cultivation was carried out from spontaneously formed nuclei with the pseudo-hexagonal morphology. During 30–35 days, optically high-quality crystals were obtained in the form of hexagonal prisms with well-developed crystallographic facets. The average growth rate was  $0.15 \pm 0.05$  mm per day. The crystal facets of the grown  $\beta$ -LAS crystals with and without the Mn impurity were identical.

In order to identify the grown crystals, an X-ray diffraction study was performed on an automatic STOE STADI diffractometer. For research, the crystals were ground to form a powder. Measurements were made in the angle interval from  $5.0^\circ$  to  $103.865^\circ$  with an increment of  $0.015^\circ$ . Diffractograms were recorded at a rate of 400 s/step. The Cu  $K\alpha$ -transition with  $\lambda = 1.54060$  Å at a voltage of 40 kV and a current of 35 mA was used as a radiation source. Measurements were carried out at a temperature of  $24.0^\circ\text{C}$ .

The thermal expansion of the crystals was studied with the use of a quartz dilatometer. The installation made it possible to examine specimens with optimal linear dimensions of about 1 cm and a maximum linear elongation of 0.1 mm. The researched specimen had the following dimensions:  $d_x = 3.79$  mm,  $d_y = 3.08$  mm, and  $d_z = 3.59$  mm. The quartz rod provided a reduction of the vertical temperature gradient between the specimen and the indicator. In order to account for the linear expansion of the quartz rod, the temperature-induced changes of the indicator readouts were measured in the presence and absence of the examined specimen and by zeroing the dilatometer readouts at room temperature in both cases. Their difference is the thermal elongation of the specimen at a given temperature. The measurement accuracy of the specimen dimensions was  $\pm 0.001$  mm. Every temperature point was held for 10–15 min.

For anisotropic crystals, the coefficient of thermal expansion is defined as a second-rank tensor. For crystals of the rhombic system, which include the examined one, it is necessary to know the expansion

coefficient values in three mutually perpendicular directions that are parallel to the second-order axes:  $\alpha_{11} = \alpha_1$ ,  $\alpha_{22} = \alpha_2$ , and  $\alpha_{33} = \alpha_3$ . The coefficient of linear thermal expansion  $\alpha_l$  is calculated according to the formula

$$\alpha_l = \frac{l - l_0}{l_0 \times (T - T_0)}, \quad \alpha_l = \frac{dl}{l_0 \times dT}. \quad (1)$$

The coefficient of volumetric thermal expansion of the crystal is the sum of all three linear coefficients,

$$\beta = \alpha_V \sim \alpha_1 + \alpha_2 + \alpha_3. \quad (2)$$

The differential thermal analysis of single crystals was carried out making use of a synchronous thermal analyzer LINSEIS STA PT1600, which allows the temperature and time dependences of changes in the heat flux and the material mass to be measured in a controlled atmosphere. Before measurements, specimens with a mass less than 100 mg were ground to a powder. Temperature studies were carried out within a temperature interval of 20–310 °C in the heating and cooling modes at a rate of 10 °C/min. The accuracy of temperature measurements was  $\pm 0.001^\circ\text{C}$ . On the basis of the obtained thermograms, which allow one to distinguish between endothermic and exothermic effects both related (the compound decay) and not related (melting and crystallization) to the weight loss, it is possible to clearly determine the temperature of the structural phase transition.

### 3. Results and Discussion

The X-ray studies of the structure made it possible to identify the phase that is stable in a temperature interval of 284–459.5 K; this is the compound  $\beta$ - $\text{LiNH}_4\text{SO}_4$ . On the basis of the crystal structure model [3, 30–33] and experimentally obtained diffraction patterns (see Fig. 1), the structure of the researched compound, atomic coordinates, and the parameters of elementary lattice were specified. Namely, the crystal belongs to the orthorhombic system and has the space symmetry group  $Pna2_1$  (No. 33); the unit cell with the parameters  $a = 8.7741(4)$  Å,  $b = 9.1251(4)$  Å, and  $c = 5.2785(3)$  Å contains four formula units ( $Z = 4$ ). Using the Rietveld method and on the basis of the experimentally determined lattice parameters, the component composition of the obtained crystals was specified, and the presence of the Mn impurity was confirmed. The inclusion of Mn

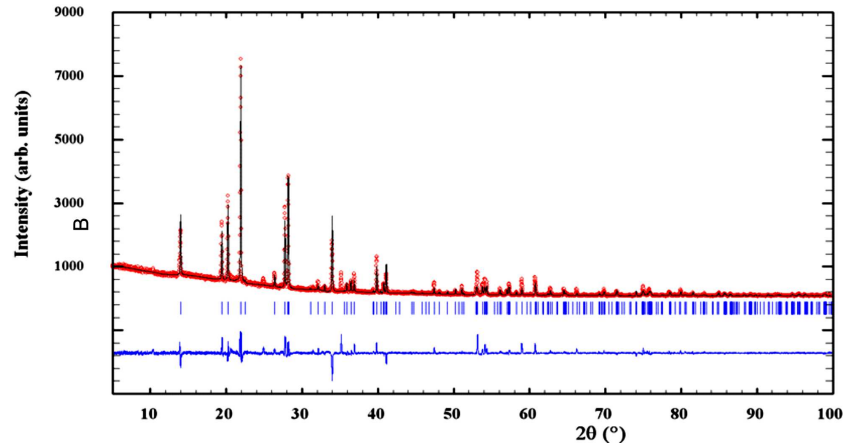


**Fig. 1.** Experimental (circles), theoretical (solid curve), and difference (bottom curve) diffraction patterns of  $\beta\text{-LiNH}_4\text{SO}_4\text{:Mn(5 wt.%)}$  specimen

into the  $\beta\text{-LiNH}_4\text{SO}_4$  structure manifests itself as a reduction of the unit cell volume  $V$  by  $0.84 \text{ \AA}^{-3}$ , i.e., to  $422.62(3) \text{ \AA}^{-3}$ . On the basis of our previous studies concerning the refractive parameters, we made an assumption about the partial substitution of Li atoms by Mn ones (heterovalent substitution of  $2\text{Li}^+$  by  $\text{Mn}^{2+}$ ).

Dilatometric studies of the crystals are a reliable experimental tool that allows the temperature and character of PT to be determined unambiguously. The results experimentally obtained for the temperature dependence of the relative elongation of Mn-doped (5 wt.%) and pure [22]  $\text{LiNH}_4\text{SO}_4$  crystals in the temperature interval of 295–495 K are presented in Fig. 2. One can see that the introduction of Mn impurity does not modify substantially the behavior of temperature expansion in three directions, but only change the absolute values of  $\Delta l/l_0$ : in the ferroelectric phase, the growth equals  $0.47 \times 10^{-3}$ ,  $0.27 \times 10^{-3}$ , and  $0.06 \times 10^{-3}$  along the  $Y$ ,  $X$ , and  $Z$  directions, respectively. A smooth, almost linear increase of the specimen size is observed along the  $Y$  and  $X$  directions as the temperature grows from room temperature to 450 K. The coefficients of linear temperature expansion in those directions are almost identical both by the sign and the absolute value. Along the  $Z$  direction, a smooth transition from an almost zero expansion of the specimen to a negative one is observed as the temperature increases, which can be distinctly seen in the PT vicinity (Fig. 2).

Negative thermal expansion (NTE) arises as a result of long-range bond forces in the crystal. These

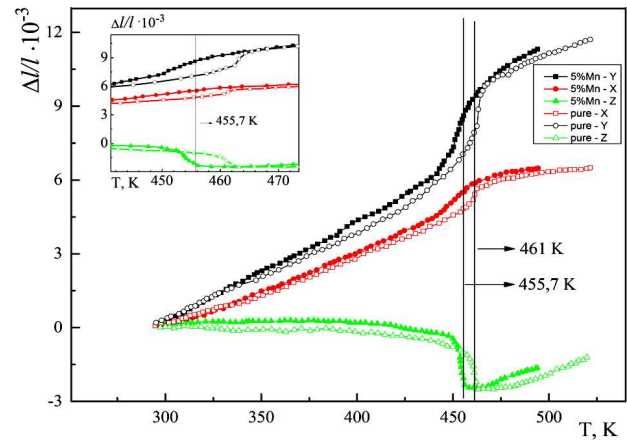


**Fig. 2.** Thermal expansion of pure and impurity-doped  $\beta\text{-LiNH}_4\text{SO}_4\text{:Mn(5 wt.%)}$  crystals

forces, which appear, when the atoms become polarized, diminish the vibration frequencies of acoustic modes in the phonon spectrum near the Brillouin-zone boundary. The values of the Grüneisen coefficient  $\gamma_i$  at those frequencies are small positive numbers for longitudinal vibrations and negative ones for transverse vibrations. As a result, the average value of this parameter decreases and can acquire negative values in a certain temperature interval [3].

It is known that the coefficient of volumetric thermal expansion of the  $\beta$ -crystal can be written in the form

$$\beta = \gamma_i \chi_T (C_V/V). \quad (3)$$

Here,  $V$  is the molar volume,  $C_V$  the molar heat capacity,  $\chi_T = -1/V (\partial V/\partial P)_T$  is the coefficient of

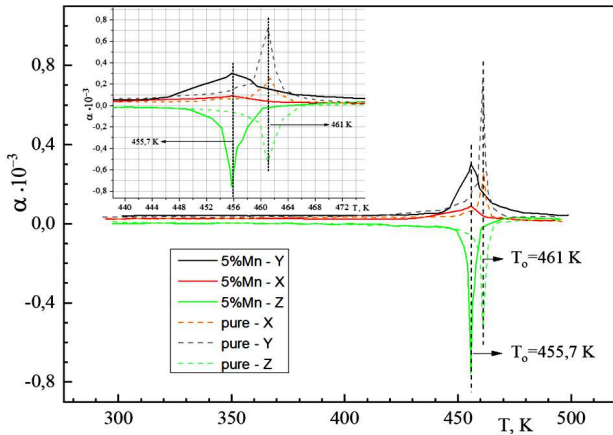


**Fig. 3.** Temperature dependences of the coefficients of linear expansion of pure and  $\beta$ -LiNH<sub>4</sub>SO<sub>4</sub> : Mn(5 wt.%) crystals. The same dependences near the phase transition point are shown in the inset

isothermal compressibility of the crystal, and  $\gamma_i = -(\partial \ln T / \partial \ln V)_S$  is the Grüneisen parameter, which characterizes the variation of the crystal temperature at the adiabatic volume change. From formula (3), we see that NTE is possible, only if the parameter  $\gamma_i$  has a negative value.

The NTE mechanism in  $\beta$ -LiNH<sub>4</sub>SO<sub>4</sub> is a result of changes in the bonds between particles when approaching the ferroelectric PT point, which, in turn, induce changes in the crystal symmetry, displacements of massive charged particles, and spontaneous polarization. The temperature behavior of the spontaneous polarization is directly responsible for the volume variation of the unit cell. The  $\beta$ -LAS crystal can be called one of the irregular ferroelectrics [16], since the spontaneous polarization increases as the temperature decreases.

NTE is also observed in the ammonium sulfate (NH<sub>4</sub>)<sub>2</sub>SO<sub>4</sub> crystal (it is isomorphic to  $\beta$ -LAS) in the ferroelectric phase along the  $\alpha$ -axis [35, 36]. Along the other two axes, the crystal has positive expansion. Above the PT point, the coefficients of thermal expansion along all directions are positive. It was experimentally found that NTE for the crystals of this sulfate group is directly related to the presence of the ferroelectric phase. For instance, the ferroelectric properties disappear at the isomorphic substitution NH<sub>4</sub>  $\rightarrow$  Rb, and no HTE is observed for the Rb<sub>2</sub>SO<sub>4</sub> crystal [29].

NTE in  $\beta$ -LiNH<sub>4</sub>SO<sub>4</sub> and (NH<sub>4</sub>)<sub>2</sub>SO<sub>4</sub> does not take place in the whole temperature interval of the ferro-

electric phase, but only in a narrow vicinity of the PT point. The studies of the temperature behavior of the birefringence [13, 14] and dielectric permittivity together with the optical observations of specimen surfaces showed that the PT begins well below  $T_o$  in nominally pure  $\beta$ -LAS crystals. A heterophase system was revealed near the ferroelectric-paraelectric phase transition point, which manifests itself as the anomalous behavior of numerous physical properties and governs the orientation of the ferroelectric domain wall [19, 20]. A drastic change of the unit cell parameters along all directions and the maximum anisotropy of the thermal expansion occur in the temperature interval of this transient phase. It was found that the introduction of the Mn impurity (5 wt.%) into the crystal substantially modifies the ratio  $\Delta l/l_0$  in the transient phase: this quantity increases by  $1.14 \times 10^{-3}$  and  $0.74 \times 10^{-3}$  along the Y- and X-directions, respectively, but it decreases by  $1.34 \times 10^{-3}$  along the Z-direction. Hence, the coefficients of thermal expansion along the Y- and X-directions are positive, and it is negative along the Z-direction:  $\alpha_X = 0.25 \times 10^{-3} \text{ K}^{-1}$ ,  $\alpha_Y = 0.69 \times 10^{-3} \text{ K}^{-1}$ , and  $\alpha_Z = -0.52 \times 10^{-3} \text{ K}^{-1}$  (Fig. 3). For the impurity-doped  $\beta$ -LAS crystal, we have the following results:  $\alpha_X = 0.08 \times 10^{-3} \text{ K}^{-1}$ ,  $\alpha_Y = 0.29 \times 10^{-3} \text{ K}^{-1}$ , and  $\alpha_Z = -0.74 \times 10^{-3} \text{ K}^{-1}$ . In the paraphase, the coefficients of linear temperature expansion are positive in all three directions; so, as the temperature increases, the unit cell volume increases as well. Therefore, the transformation of the thermal expansion from negative to positive is a consequence of the spontaneous polarization disappearance. In particular, for impurity-doped crystals in the paraphase, we have almost identical growth of  $\Delta l/l_0$  along all directions in comparison with pure crystals:  $0.34 \times 10^{-3}$ ,  $0.33 \times 10^{-3}$ , and  $0.47 \times 10^{-3}$  along the directions Y, X, and Z, respectively.

Figure 3 demonstrates the temperature dependence, and Fig. 4 shows the spatial distribution of the thermal expansion coefficient  $\alpha_i$  for a Mn-doped  $\beta$ -LiNH<sub>4</sub>SO<sub>4</sub> crystal, which were plotted on the basis of experimentally obtained dependences  $\Delta l/l_0(T)$ . As one can see, distinct peaks are observed in the  $\alpha_i(T)$  dependence in the PT vicinity, which confirms the presence of PT in the pure and impurity-doped crystals. Furthermore, in the interval of positive thermal expansion, the introduction of the impurity leads to a reduction of the  $\alpha_i$ -value at the PT:  $\alpha_i \approx 7.1 \times 10^{-4}$

for the pure crystal and  $\alpha_i \approx 1.2 \times 10^{-4}$  for the impurity-doped one. At the same time, the opposite effect takes place in the NTE interval, i.e., the absolute value of  $\alpha_i$  increases, if the impurity is introduced: from about  $5.0 \times 10^{-4}$  for the pure crystal to about  $7.8 \times 10^{-4}$  for the impurity-doped one. One can also see that the doping extends the temperature interval of NTE existence from about 8 K to about 10 K.

From Fig. 4, one can see that, in the ferroelectric phase, the indicative surface of the thermal expansion coefficient at room temperature has the form of a toroid elongated along the  $Y$ -direction, and, as the temperature increases, along the  $X$ -direction. All 3D figures demonstrate a smooth transition of the thermal expansion coefficient along the  $Z$ -direction from zero to a definitely negative value (the red region) at  $T = 450$  K. In the paraphase ( $T = 475$  K), the thermal expansion coefficients along all axes are positive: the indicative surface of the thermal expansion coefficient has the form of a toroid elongated along the  $Z$ -direction.

The introduction of the Mn impurity forces the PT point to shift toward lower temperatures. At the temperature  $T_c = 455.7$  K, the  $\beta$ -LAS:Mn (5 wt.%) crystals (5 wt.%) undergo the second-kind PT “ferroelectric phase–paraelectric phase” (in the pure crystal, the PT occurs at 461 K). Such a shift can be a consequence of internal stresses that arise, if an impurity with a different atomic radius is introduced: their directionality can prevent the temperature-induced rotation of  $(\text{SO}_4)^{2-}$  tetrahedra. In this case, the ferroelectric PT, which gives rise to the symmetry change and the appearance of spontaneous polarization, takes place at lower temperatures. In turn, this leads to a shift of the temperature interval, where the transient phase exists and, therefore, the temperature interval with NTE toward lower temperatures.

In order to additionally verify the presence of a phase transition in the impurity-doped LAS crystal, we performed its differential thermal analysis (DTA) in the heating and cooling modes using a synchronous thermal analyzer LINSEIS STA PT 1600. The DTA is known to be one of the most common methods for registering and studying PTs (their thermal effects) and the intervals of compound stability. The DTA curve was obtained for the SK specimen preliminary annealed at the temperature  $T = 400$  K. The heating and cooling rates were equal to 10 K/min. The DTA results obtained for the lithium-ammonium sul-

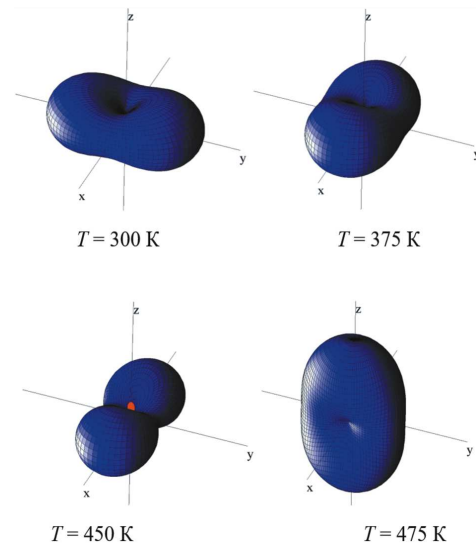


**Fig. 4.** Spatial distribution of the coefficient of thermal expansion  $\alpha$  for Mn-doped  $\beta$ - $\text{LiNH}_4\text{SO}_4$  crystal

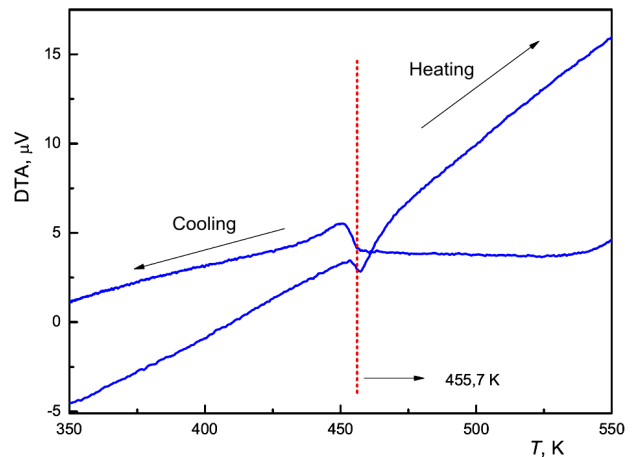


**Fig. 5.** DTA curves registered in the heating and cooling modes for doped  $\beta$ - $\text{LiNH}_4\text{SO}_4$ :Mn(5 wt.%) crystals in the vicinity of phase transition

fate compound (Fig. 5) showed its existence up to a temperature of 550 K.

To unambiguously study the PT point shift, DTA measurements were performed in two modes: heating and cooling within the temperature interval of 294–550 K. From the figure, one can see that, in the case of heating, the endothermic effect is observed in the interval of 450–460 °C. A distinct peak was detected at a temperature of 455.9 K in the case of heating, and at 454.1 K in the case of cooling. The obtained

DTA results confirmed the presence of phase transformations in the impurity-doped lithium-ammonium sulfate compound, as well as the corresponding shift of the PT point in the case of doping.

#### 4. Conclusions

In this work, the influence of the transition metal impurity (manganese) on the thermal properties of lithium-ammonium sulfate crystals in the temperature interval from room temperature to 555 K has been studied.

The indicated compound has been synthesized, and its structure, the atomic coordinates, and the parameters of the unit cell have been specified. The crystal belongs to the orthorhombic system and has the space symmetry group  $Pna2_1$ . The unit cell ( $a = 8.7741(4)$  Å,  $b = 9.1251(4)$  Å, and  $c = 5.2785(3)$  Å) contains four formula units ( $Z = 4$ ). The doping decreases the unit cell volume because Mn atoms, whose atomic radius is smaller, partially replace Li ones.

It has been found that the introduction of the Mn impurity does not significantly change the behavior of the crystal temperature expansion, but only leads to a variation of the absolute values of the ratio  $\Delta l/l_0$ . In the ferroelectric phase, we observe a smooth almost linear increase of the specimen sizes along the  $Y$ - and  $X$ -direction as the temperature grows from room temperature to 450 K, and a smooth transition from an almost zero expansion of the specimen size to a negative one in the  $Z$ -direction, which is clearly observed near the PT.

The introduction of the Mn impurity (to 5 wt.%) leads to a PT shift toward lower temperatures: from 461 K for the pure crystal to 455.7 K for the impurity-doped one. This is a result of internal stresses that arise, if an impurity with a different atomic radius is introduced, and whose directionality prevents the temperature-induced rotation of  $(\text{SO}_4)^{2-}$  tetrahedra.

It has been found that, in the interval of positive thermal expansion, the impurity introduction leads to a reduction of the linear expansion coefficient  $\alpha_i$ , whereas, in the interval of negative thermal expansion, the effect is opposite: the absolute value of  $\alpha_i$  increases. The introduction of the impurity also gives rise to an extension of the temperature interval of NTE from about 8 K to about 10 K.

The indicative surfaces of the thermal expansion coefficient in the ferroelectric and paraelectric phases have been plotted. This will allow an impurity-doped

LAS crystal to be used as a compound with NTE in functional materials of various types. First of all, this is important for their practical applications, since most of the existing industrial-grade materials have a positive coefficient of thermal expansion, which negatively affects their performance at temperatures higher than “extreme” ones.

1. P. Tomaszewski. Polytypism of  $\alpha$ - $\text{LiNH}_4\text{SO}_4$  crystals. *Solid State Commun.* **81**, 333 (1992).
2. A. Pietraszko, K. Lukaszewicz. Crystal structure of  $\alpha$ - $\text{LiNH}_4\text{SO}_4$  in the basic polytypic modification. *Pol. J. Chem.* **66**, 2057 (1992).
3. H. Mashiyama, H. Kasano. Refined crystal structure of  $\text{LiNH}_4\text{SO}_4$  including hydrogen atoms in phases II and III. *J. Phys. Soc. Jpn.* **62**, 155 (1993).
4. X. Solans, J. Mata, M.T. Calvet, M. Font-Bardia. X-ray structural characterization, Raman and thermal analysis of  $\text{LiNH}_4\text{SO}_4$  above room temperature. *J. Phys: Condens. Matter.* **11**, 8995 (1999).
5. M. Polomska, B. Hilczer, J. Baran. FIR studies of  $\alpha$  and  $\beta$  polymorphs of  $\text{LiNH}_4\text{SO}_4$  single crystals. *J. Mol. Struct.* **325**, 105 (1994).
6. M.Ya. Rudysh, V.Yo. Stadnyk, R.S. Brezvin, P.A. Shchepanskyi. Energy band structure of  $\text{LiNH}_4\text{SO}_4$  crystals. *Phys. Solid State* **57**, 53 (2015).
7. V.I. Stadnyk, R.S. Brezvin, M.Ya. Rudysh, P.A. Shchepanskyi, V.M. Gaba, Z.A. Kogut. On isotropic states in  $\alpha$ - $\text{LiNH}_4\text{SO}_4$  crystals. *Opt. Spectrosc.* **117**, 756 (2014).
8. N.P. Sabalisk, C. Guzmán-Afonso, C. González-Silgo, M.E. Torres, J. Pasán, J. del-Castillo, D. Ramos-Hernández, A. Hernández-Suárez, L. Mestres. Structures and thermal stability of the  $\alpha$ - $\text{LiNH}_4\text{SO}_4$  polytypes doped with  $\text{Er}^{3+}$  and  $\text{Yb}^{3+}$ . *Acta Crystallogr. B* **73**, 122 (2017).
9. D. Komornicka, M. Wolczyr, A. Pietraszko. Polymorphism and polytypism of  $\alpha$ - $\text{LiNH}_4\text{SO}_4$  crystals. Monte Carlo modeling based on X-ray diffuse scattering. *Cryst. Growth Des.* **14**, 5784 (2014).
10. T.I. Chekmasova, I.P. Aleksandrova. NMR investigation of the high-pressure phase in  $\text{LiNH}_4\text{SO}_4$ . *Phys. Status Solidi A* **49**, K185 (1978).
11. B.O. Hildmann, Th. Hahn, L.E. Crossand, R.E. Newnham. Lithium ammonium sulphate, a polar ferroelastic which is not simultaneously ferroelectric. *Appl. Phys. Lett.* **27**, 103 (1975).
12. M.A. Gaffar, A. Abu El-Fadl. Electric, dielectric and optical studies of the lower phase transition of lithium ammonium sulphate single crystals. *Physica B* **262**, 159 (1999).
13. M.Ya. Rudysh, V.Yo. Stadnyk, P.A. Shchepanskyi, R.S. Brezvin, J. Jedryka, I.V. Kityk. Specific features of refractive, piezo-optic and nonlinear optical dispersions of  $\beta$ - $\text{LiNH}_4\text{SO}_4$  single crystals. *Physica B* **508**, 411919 (2020).
14. M.Y. Rudysh, M.G. Brik, O.Y. Khyzhun, A.O. Fedorchuk, I.V. Kityk, P.A. Shchepanskyi, V.Y. Stadnyk, G. Lakshminarayana, R.S. Brezvin, Z. Bak, M. Piasecki. Ionicity and birefringence of  $\alpha$ - $\text{LiNH}_4\text{SO}_4$  crystals: ab-initio DFT

- study and X-ray spectroscopy measurements. *RSC Adv.* **7**, 6889 (2017).
15. S. Hirotsu, Y. Kunii, I. Yamamoto, M. Miyamoto, T. Mitsui. Brillouin scattering study of the ferroelectric phase transition in  $\text{NH}_4\text{LiSO}_4$ . *Phys. Soc. Jpn.* **50**, 3392 (1981).
  16. V.Yo. Stadnyk, R.S. Brezvin, M.Ya. Rudysh, P.A. Shchepanskyi, V.Yu. Kurlyak. Piezooptic properties of  $\text{LiNH}_4\text{SO}_4$  crystals. *Crystallogr. Rep.* **60**, 388 (2015).
  17. M. Polomska, W.Schranz, J. Wolak. Pretransitional effect below the ferroelectric–paraelectric phase transition in  $\beta$ - $\text{LiNH}_4\text{SO}_4$ . *J. Phys.: Condens. Matter* **11**, 4275 (1999).
  18. M.T. Sebastian, R.A. Becker, H. Klapper. X-ray diffraction study of lithium hydrazinium sulfate and lithium ammonium sulfate crystals under a static electric field. *J. Appl. Cryst.* **24**, 1015 (1991).
  19. T. Mitsui, T. Oka, Y. Shiroshi, M. Takashigi, K. Ito, S. Sawada. Ferroelectricity in  $\text{NH}_4\text{LiSO}_4$ . *J. Phys. Soc. Jpn.* **39**, 845 (1975).
  20. M. Polomska, N.A. Tikhomirova. Domain structure of  $\text{LiN}/\text{H,D}/_4\text{SO}_4$  revealed by liquid crystal decoration. *Ferroelectrics Lett.* **44**, 205 (1982).
  21. S. Krishnan, S.J. Raj, R. Robert, S. Ramanand, A.J. Das. Mechanical, theoretical and dielectric studies on ferroelectric lithium ammonium sulphate (LAS) single crystals. *Solid State Electron.* **52**, 1157 (2008).
  22. J. Chen, L. Hu, J. Deng, X. Xing. Negative thermal expansion in functional materials: controllable thermal expansion by chemical modifications. *Chem. Soc. Rev.* **44**, 3522 (2015).
  23. B.C. Venkata Reddy, G. Sankaiz Kupak, I. Aruna Kunari. Electronic absorption spectrum of  $\text{Cu}^{2+}$  ions doped in lithium ammonium sulphate crystal. *Ferroelectrics Lett.* **7**, 43 (1987).
  24. M. Gaafar, M.E. Kassem, S.H. Kandil. Phase transition in lithium ammonium sulphate doped with cesium metal ions. *Solid State Commun.* **115**, 509 (2000).
  25. M.A. Gaffar, A. Abu El Fadl, A. Galal Mohamed. Specific heat and electrical resistivity of pure and doped lithium-ammonium sulphate single crystals. *Physica B* **217**, 274 (1996).
  26. M.A. Gaffar, Galal A. Mohamed, A. Abu El-Fadl, A.M. Mebed. Thermal properties of pure and doped lithium-ammonium sulphate single crystals. *Physica B* **205**, 224 (1995).
  27. A. Hadni, R. Thomas. Observation of domain wall motions in alanine doped triglycine sulphate ferroelectric crystal. *Appl. Phys.* **10**, 91 (1976).
  28. A. Hadni, R. Thomas. Localized irreversible thermal switching of spontaneous polarization in ferroelectrics by laser. *Ferroelectrics* **7**, 87 (1974).
  29. U. Robels, J.H. Calderwood. Shift and deformation of the hysteresis curve of ferroelectrics by defects: An electrostatic model. *J. Appl. Phys.* **77**, 4002 (1995).
  30. R.B. Matviiv, M.Ya. Rudysh, V.Yo. Stadnyk, A.O. Fedorchuk, P.A. Shchepanskyi, R.S. Brezvin, O.Y. Khyzhun. Structure, refractive and electronic properties of  $\text{K}_2\text{SO}_4:\text{Cu}^{2+}$  (3%) crystals. *Curr. Appl. Phys.* **21**, 80 (2021).
  31. V.Yo. Stadnyk, R.B. Matviiv, M.Ya. Rudysh, R.S. Brezvin, P.A. Shchepanskyi, B.V. Andrievskii. Refractive parameters and band energy structure of  $\text{K}_2\text{SO}_4$  crystals doped with copper. *J. Appl. Spectrosc.* **87**, 143 (2020).
  32. O.S. Kushnir, P.A. Shchepanskyi, V.Yo. Stadnyk, A.O. Fedorchuk. Relationships among optical and structural characteristics of  $\text{ABSO}_4$  crystals. *Opt. Mater.* **95**, 109221 (2019).
  33. M.O. Romanyuk. *Workshop on Crystal Optics and Crystal Physics* (Lviv Nat. Univ., 2012) (in Ukrainian).
  34. S.I. Novikova. *Thermal Expansion of Solids* (Nauka, 1974) (in Russian).
  35. I.M. Shmytko, N.S. Afonikova, V.I. Torgashev. Anomalous states of the structure of  $(\text{NH}_4)_2\text{SO}_4$  crystals in the temperature range 4.2–300 K. *Phys. Solid State* **44**, 2309 (2002).
  36. I.M. Shmytko, N.S. Afonikova, V.I. Torgashev. Anomalous states of the crystal structure of  $(\text{Rb}_{0.1}(\text{NH}_4)_{0.9})_2\text{SO}_4$  solid solutions in the temperature range 4.2–300 K. *Phys. Solid State* **44**, 2165 (2002).

Received 25.05.22.

Translated from Ukrainian by O.I. Voitenko

Р.С. Брезвін, О.Я. Костецький,  
В.Й. Стадник, П.А. Щепанський,  
О.М. Горіна, М.Я. Рудши, А.О. Шапранський

#### ДИЛАТОМЕТРИЧНІ ДОСЛІДЖЕННЯ КРИСТАЛІВ $\text{LiNH}_4\text{SO}_4$ З ДОМІШКОЮ МАРГАНЦЮ

Синтезовано кристал літій-амоній сульфату з домішкою марганцю Mn (5%) та уточнено його структуру (координати атомів та параметри елементарної ґратки). Встановлено, що введення домішки призводить лише до зміни абсолютних значень термічного розширення  $\Delta l/l_0$ , не змінюючи його характеру, притому вздовж напрямку  $Z$  в околі точки фазового переходу виявлено негативне термічне розширення. Показано, що введення домішки приводить до зміщення точки фазового переходу в бік нижчих температур з 461 К (для чистого) до 455,7 К (для домішкового), до зменшення величини коефіцієнта лінійного розширення  $\alpha_i$  в області позитивного термічного розширення, та його збільшення в області негативного термічного розширення, а також спричиняє зростання температурного інтервалу існування ділянки негативного термічного розширення. Побудовано вказівні поверхні коефіцієнта термічного розширення в сегнето- та параелектричній фазах. Проведено незалежне вивчення та підтвердження фазового переходу методом диференціального термічного аналізу.

**Ключові слова:** кристал, домішка, термічне розширення, фазовий перехід, диференціальний термічний аналіз.